



# Laser Beam Propagation Features via Atmospheric Turbulence-Induced Beam Wander: Testbed Conceptual Design

Haider M Al Juboori, James Garland

## ► To cite this version:

Haider M Al Juboori, James Garland. Laser Beam Propagation Features via Atmospheric Turbulence-Induced Beam Wander: Testbed Conceptual Design. COAT-2023 - workshop (Communications and Observations through Atmospheric Turbulence), Mar 2023, Durham (GB), United Kingdom. hal-04246206

**HAL Id: hal-04246206**

**<https://hal.science/hal-04246206v1>**

Submitted on 17 Oct 2023

**HAL** is a multi-disciplinary open access archive for the deposit and dissemination of scientific research documents, whether they are published or not. The documents may come from teaching and research institutions in France or abroad, or from public or private research centers.

L'archive ouverte pluridisciplinaire **HAL**, est destinée au dépôt et à la diffusion de documents scientifiques de niveau recherche, publiés ou non, émanant des établissements d'enseignement et de recherche français ou étrangers, des laboratoires publics ou privés.

# Laser Beam Propagation Features via Atmospheric Turbulence-Induced Beam Wander: Testbed Conceptual Design

Haider M. Al-Juboori<sup>\*a</sup>, James Garland<sup>a</sup>

<sup>a</sup> Dept. of Electronics Engineering and Communications, Faculty of Engineering, South East Technological University, Carlow, Ireland

## ABSTRACT

One of the promising technologies for sending high data rates over long distances with compact antennas and low power usage is optical free-space communications (OFSC). The high-speed links between satellites, up- and down-links from and to ground stations, and other links between aeronautical vehicles or in deep space communications (DSC) are all potential scenarios for future applications.

Various effects severely degrade the signal and capabilities of OFSC, such as laser beam spreading, wandering and scintillation. The first part of our study discusses the emulation concepts of wandering impact. Then, we use the PILab numerical simulation platform to visualize the effective parameters and simulate atmospheric optical propagation especially for wandering effect.

Noteworthy, machine learning (ML) algorithms have recently been considered promising approaches for solving high-order nonlinear equations and comparing the activation function for high-order equations. We propose a laboratory testbed with a novel wavefront aberration compensation technique using Machine Learning, especially ML have a good chance to support developing and testing processes related to adaptive nonlinear characterization for OFSC systems.

The turbulence generator's development, the testbed's concept, and its optical design are illustrated. The conceptual principles of the testbed make it possible to reproduce test scenarios with realistic ratios of aperture size over the Fried parameter.

**Keywords:** Modelling and simulation for OFSC, emulation GEO satellite links, atmospheric turbulence impact and mitigation.

## 1. INTRODUCTION

A coherent laser beam traveling through the atmosphere from satellite-to-ground (downlink) or ground-to-satellite (uplink) confronts unique restrictions. These restrictions include absorption, scattering effects, and cloud impact as a blocking barrier that creates turbulence-induced wavefront distortions. The major challenge in free-space communications is atmospheric turbulence, especially in an altitude range of 20 km height, between the Tropopause atmospheric layer and ground level, as Figure 1 explains.

The water particles, under various weather patterns such as fog, rain, and snow, presented along the propagation channel will cause fading. Significant sources of atmospheric absorption and scattering phenomena that impact laser beam propagation are free aerosol particles in the earth's atmosphere and diverse gas molecules. The periodic daily heating and cooling of the earth's surface cause energy to be transferred to the air, which creates a random motion and causes turbulence [1]. Known as eddies, large-scale spatial motion progressively fragments into smaller air pockets of arbitrary dimensions and temperatures. The propagated wavefront of the laser beam localized changes in amplitude and phase as it passes through these eddies because the air refractive index is altered by temperature fluctuations.

Eddies bigger than the laser beam size cause random deviation of the propagation direction, known as beam wander  $\rho^2_l$ . This phenomenon is a significant issue in uplinks because changes in the beam trajectory at the start of the journey cause displacements of several hundred meters at the position of the receiving satellite.

---

<sup>\*</sup> [haider.aljuboori@setu.ie](mailto:haider.aljuboori@setu.ie) ; phone: +353 (0) 59 91 75000; [setu.ie/haider](http://setu.ie/haider)

This wandering of the beam results in a slowly fluctuating extensive dynamic range of the received signal intensity since the receiver aperture diameter is often small-scale and considered a point source receiver. The received wavefront is distorted by beam spreading, which results when the eddies are smaller than the beam size and cause diffraction and scattering.

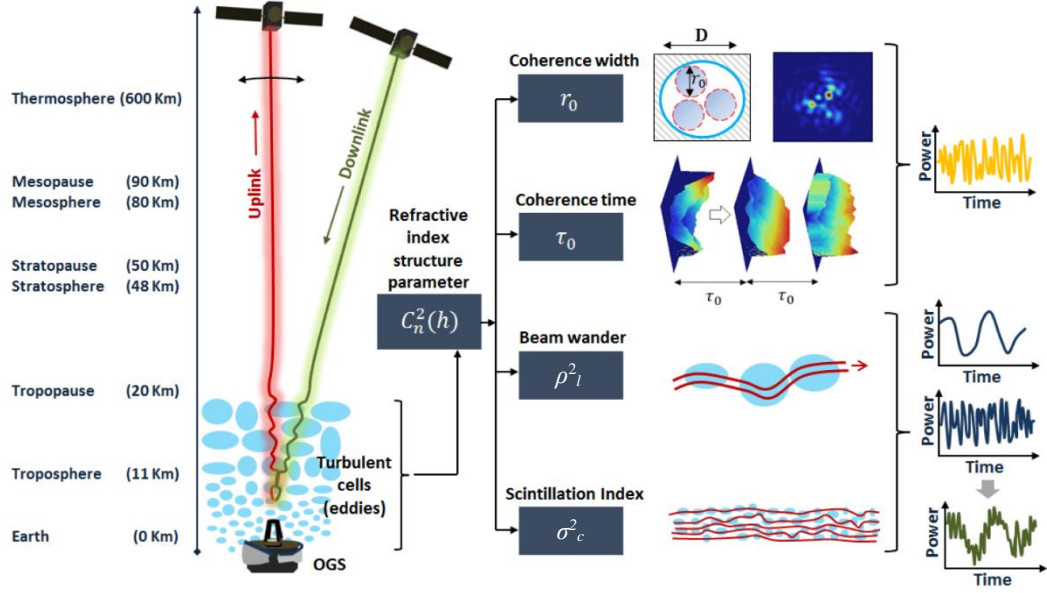


Figure 1. The most known resources of atmospheric turbulence on the optical uplink/downlink [1].

Several analytical studies [2], [3], [4] and experimental research [5], [6], [7] were conducted to understand and reduce the turbulence effect on OFSC systems, and many solutions were suggested.

For the simulation of the fluctuations of the refractive index in the present work, the method used random phase screens that alter the photon distribution function, which describes the photon's behavior. Beam wandering was simulated and compared for three different elevation angles for 40,000 km propagation distances under ground-level turbulence  $C_n^2 \approx 1.7 \times 10^{-14} \text{ m}^{-2/3}$ .

## 2. METHODOLOGY

One of the most critical variables for investigating laser beam propagation in the atmosphere is the propagation channel's refractive index (RI). Turbulence causes random temperature oscillations, leading to variations in the medium's RI. The relationship between pressure, temperature and RI ( $n$ ) at a location  $r$  in space can be described as [8]:

$$n(r) = 1 + 79 \times 10^{-6} \frac{P(r)}{T(r)} \quad \dots(1)$$

Where  $T$  is the temperature in Kelvin, and  $P$  is the pressure in millibars. The change in RI is mainly caused by temperature fluctuation due to the negligible pressure variation (hypothetically). The refractive index structural parameter  $C_n^2$  ( $\text{m}^{-2/3}$ ) values determine how extensively the turbulence may be categorized into three regimes. The three regimes can be used to classify turbulence [9]:

$$\begin{aligned} C_n^2 &\geq 10^{-13} \rightarrow \text{Strong turbulence} \\ 10^{-16} &< C_n^2 < 10^{-13} \rightarrow \text{Moderate turbulence} \\ C_n^2 &\geq 10^{-16} \rightarrow \text{Weak turbulence} \end{aligned}$$

Theoretically, the degree of freedom parameter  $1/3 \times ((C_n^2)^{-2/3} \times \lambda)^{1/2}$  for the eddy size,  $R$ , is considered to be Chi-Square distributed [10,11]. Additionally, the Gamma distribution is usually used for moderate and high turbulence regimes. Figure 2 displays the eddy size ( $R$ ) in Chi-Square and Gamma distributions for a given turbulence value. Large-scale eddies

are primarily responsible for the beam wander phenomenon. Compared to the Chi-Square distribution, the mean magnitude of the eddies produced by the Gamma distribution is significant. In comparison to Chi-Square distribution, Gamma distribution exhibits very few instances of small-scale eddies in conditions of strong turbulence, making Gamma appropriate for the distribution of eddy size.

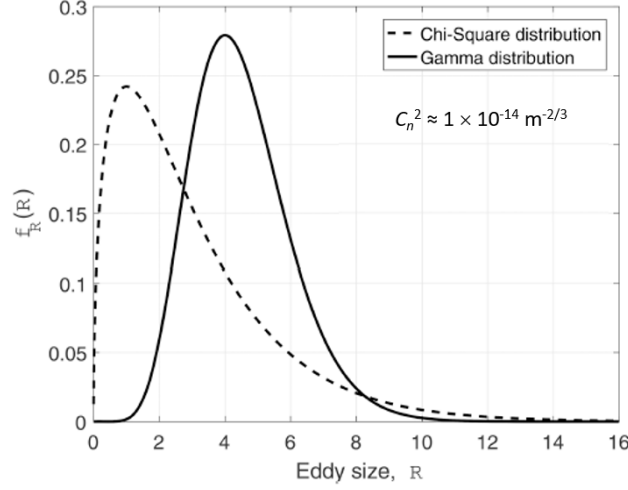


Figure 2. Chi-Square and Gamma distributions for eddy size,  $R$  [12].

For a random variable  $x$ , the probability density functions (PDF) for Gamma distribution is given by [12]

$$f_x(x; s, \theta) = \frac{x^{(s-1)} e^{-\frac{x}{\theta}}}{\theta^s \Gamma(s)}, 0 < x < \infty \text{ and } s, \theta > 0 \quad \dots(2)$$

Where  $s$  and  $\theta$  are the shape and scale parameters of the distribution, respectively, and  $\Gamma(\cdot)$  denotes the Gamma function.

We assume the centers of the turbulent eddies follow a uniform distribution within a circle of radius  $R$  centered at the propagation axis. Then, we simulate the effect of how the beam wanders under various case scenarios. A beam encounters the maximum number of turbulent eddies in these scenarios for a given propagation distance and turbulence condition.

A laser beam's divergence in free space is roughly represented by the ratio  $\lambda/D$ , where  $D$  is the transmit aperture diameter and  $\lambda$  is the laser beam's wavelength. Eddies greater than the beam diameter tend to deflect the beam when there is turbulence. In contrast, smaller eddies tend to spread the beam [13].

The beam spot wanders in the aperture plane of the receiver if the exposure time is much less than the time,  $\delta t$ , where  $\delta t = D/|v|$  and  $v$  is the transverse wind velocity. The beam form is almost identical to that of free space.

If the exposure time is much larger than  $\delta t$ , we would see a single beam spot with a larger diameter, as shown in Figure 3(a) [14]. There are, on average,  $L/2R$  eddies encountered by the propagating beam for a horizontal terrestrial link of length  $L$ . The mean square radius of beam wander is given by [15]:

For  $L < L_i$

$$\langle \rho_l^2 \rangle = \frac{\omega_0^2}{2} [(\alpha_r L)^2 + (1 + \alpha_i L)^2] + \frac{4 L^2}{k^2 \rho_0^2} \quad \dots(3a)$$

and, for  $L \geq L_i$

$$\langle \rho_l^2 \rangle = \frac{\omega_0^2}{2} [(\alpha_r L)^2 + (1 + \alpha_i L)^2] + 2.2 C_n^2 l_o^{-1/3} L^3 \quad \dots(3b)$$

Where  $w_0$  = beam radius,  $\alpha_r = \lambda/\pi w_0^2$ ,  $\alpha_i = 1/F_0$ ,  $k = 2\pi/\lambda$ ,  $L_i = (0.39k^2 C_n^2 l_0^{5/3})^{-1}$ ,  $F_0$  = focal length of the Gaussian beam, and coherence length,  $\rho_0 = (0.55k^2 L C_n^2)^{-3/5}$ .

The last two terms in (3a) and (3b) represent the impacts of air turbulence, whereas the first two terms in (3a) and (3b) represent beam spread in free space. Most of the time, condition (3a) is met. However, condition (3b) is applicable under extreme turbulence. Experimental data [14] validate (3a) and (4b) requirements. Similar analytical conclusions are also mentioned in [16] for beam wander analysis in a ground station-satellite uplink and [17] for a focused Gaussian beam in a horizontal trajectory.

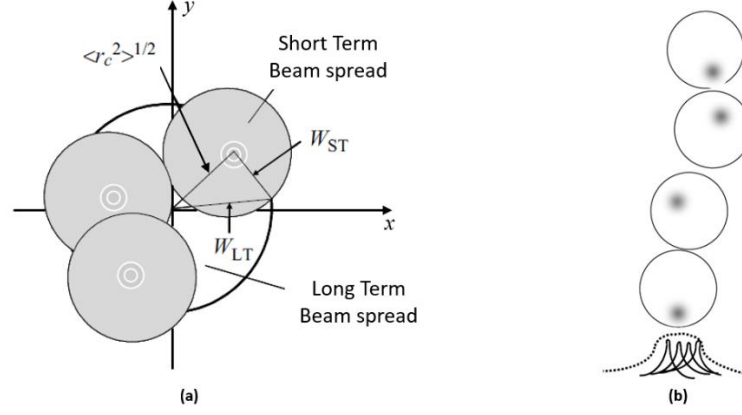


Figure 3. Beam wander effect. (a) The long-term spot size results from beam-wandering, beam breathing, and diffraction (the shaded circles depict the random motion of the short-term beam in the receiver plane). (b) The beam wanders as displacement of the beam's "hot spot" (instantaneous center) [8].

### 3. RESULTS

We used PILab code [18,19] (developed by DLR's Institute of Communications and Navigation) to simulate the beam wander effect at  $\lambda = 1550$  nm for a vertical terrestrial link length  $L$  of 40,000 km and beam waist = 50 mm use Standard Hufnagel-Vally Day (HUFVAL 5/7). More details of other parameter definitions can be found in Table 1.

Table 1: Parameters values of uplink simulation scenario.

<b>Turbulence inner scale (<math>l_0</math>) [m]</b>	$1 \cdot 10^{-5}$
<b>Turbulence outer scale (<math>L_0</math>) [m]</b>	10
<b>Beam waist [m]</b>	$5 \cdot 10^{-2}$
<b>Pseudowind (<math>v</math>) [m/s]</b>	21
<b>Ground level turbulence [<math>m^{-2/3}</math>]</b>	$1.7 \cdot 10^{-14}$
<b>Turbulence Model</b>	Kolmogorov
<b>No. of realization</b>	1000

In a moderate turbulence regime, Figure 4 shows the distribution of beam peaks throughout the aperture area using the suggested model at three different elevation angles ( $\theta_{elev}$ ). Due to turbulence-induced beam wander, beam peaks are unpredictably displaced away from the aperture's center. The effect of beam wander caused by air turbulence is more noticeable the further away the beam peaks are from the center of the receiver aperture. Figure 5 illustrates the dataset and mean radial displacement ( $R_c$ ) values for 1000 realizations at three different elevation angles ( $\theta_{elev} = \pi/i$ , and  $i = 6, 4$  and  $2$  respectively).

For each simulation elevation angle, the intensity variations of the received signal that are caused by air turbulence and the beam wander effect have been computed using PDF, see Figure 6. The results tend to match the distribution of eddies based on the Gamma model explained in Figure 2.

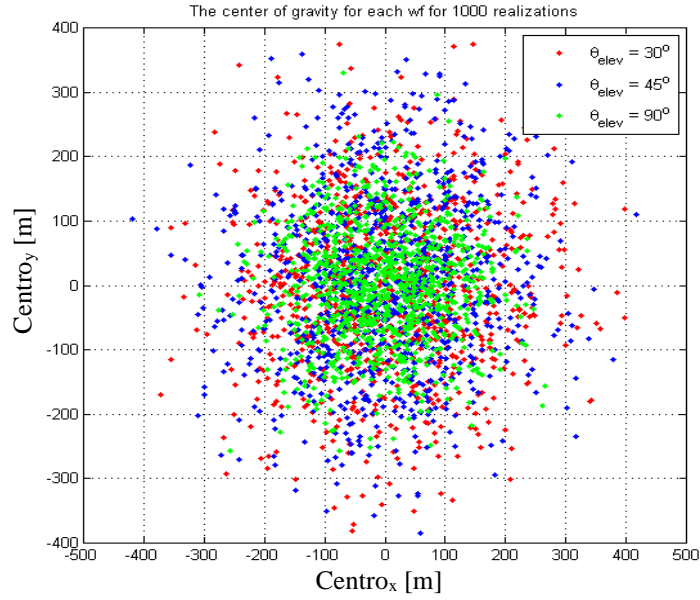


Figure 4. Random beam wandering and distribution of beam peaks over the receiver aperture (uplink simulation scenario).

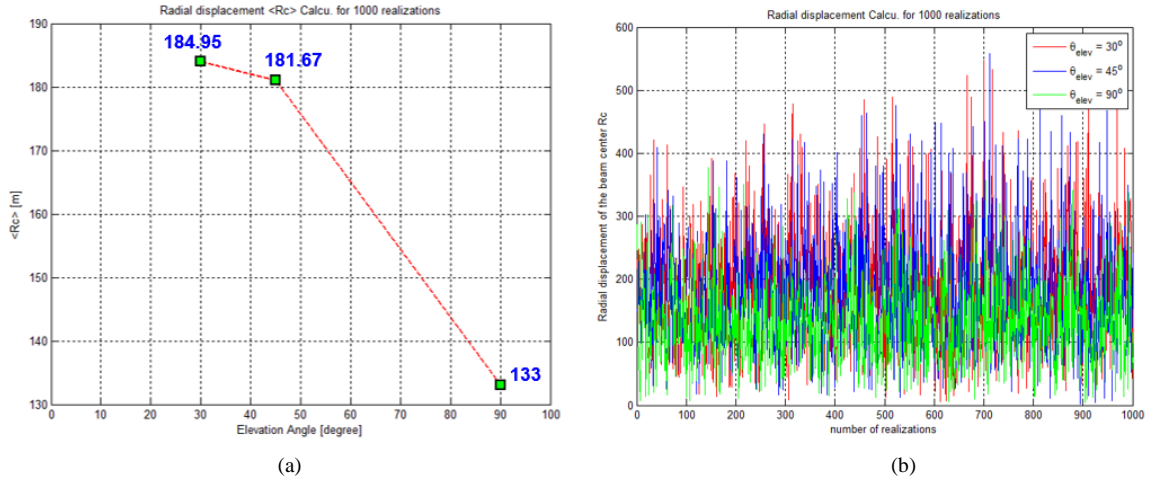


Figure 5. Simulation results of beam wandering based on PILab Code for three different elevation angles: (a) the mean value of radial displacement  $\langle R_c \rangle$ , and (b) the datasets of radial displacement values.

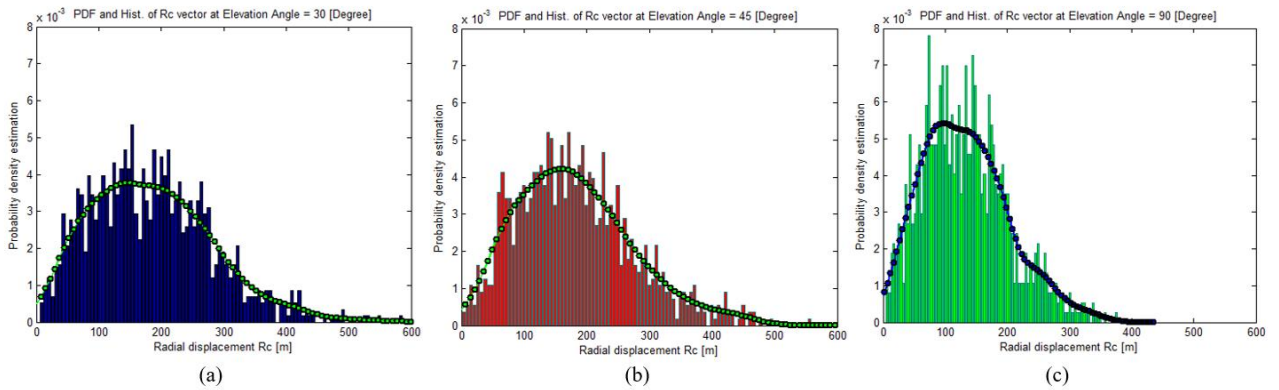


Figure 6. Probability density estimations at (a)  $\theta_{elev} = 30^\circ$ , (b)  $\theta_{elev} = 45^\circ$ , (c)  $\theta_{elev} = 90^\circ$ , respectively.

Figure 7 shows our conceptual design and laboratory-based measurement system. The beam wander is spatially modeled by a Gaussian distribution characterized by a long-term average radial variance,  $\langle r_c^2 \rangle$ , and the size of the received beam without any averaging (the short-term beam), denoted by  $W_{ST}$ , illustrated in Figure 3(a). According to the central limit theorem, we assume that a smaller short-term beam wanders about a receiving aperture and results in a larger long-term beam of Gaussian shape [14]. The size of the long-term beam can be given by  $W_{LT}^2 = W_{ST}^2 + \langle r_c^2 \rangle$  and is explained in Figure 3(a).

As demonstrated in Figure 7, a telescope can be used to magnify and condense the sent and received laser beams. The beams are captured onto a fast camera at the Fourier plane. Finally, we use a camera to measure the received beam to identify the beam's spatial movement for approximately ten seconds. As the movement of the beam must be recorded without information being lost, the camera's frame rate is a crucial factor in this experiment. This can help to systematically record the laser intensity profile and read the appropriate datasets based on synchronized changed parameters from the testbed and related and recorded images from the camera. The testbed architecture, ML algorithm, and conceptualization of multi-feature sensors will be documented and published in future work with digital analytical techniques.

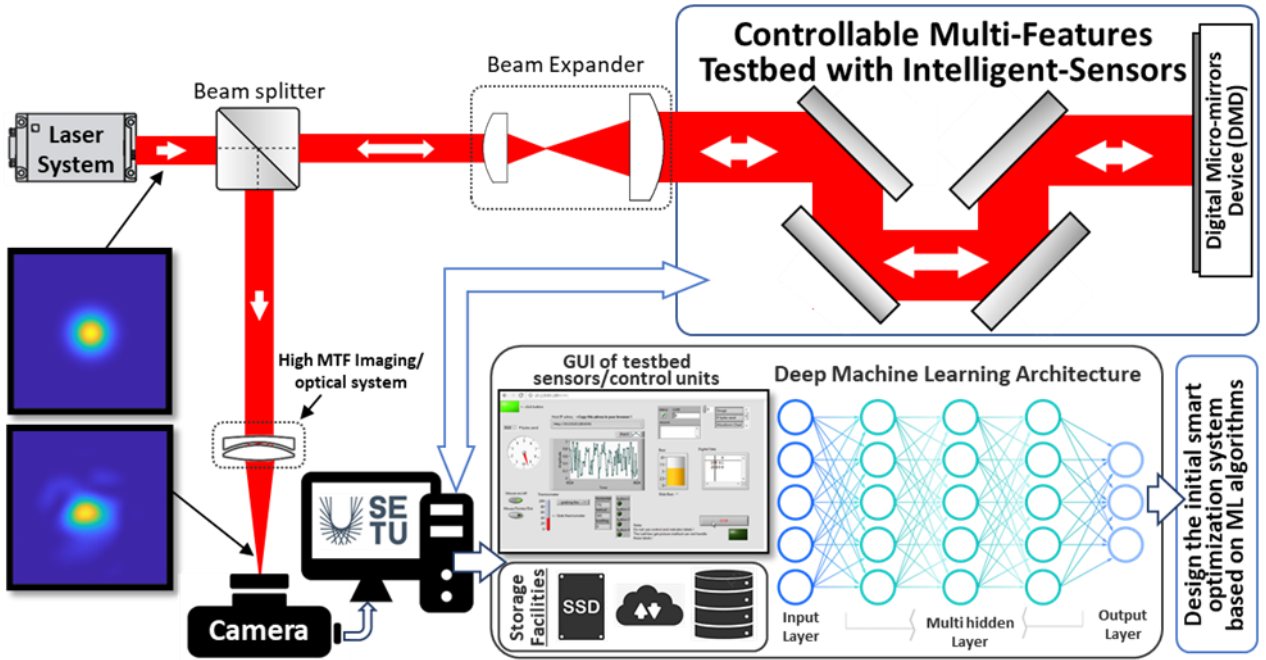


Figure 7. Future Work: diagram of the suggested ML setup in a simplified form, with insets showing beam density distribution at transmitter/receiver.

## 4. CONCLUSIONS

Scintillation, beam wandering, and phase-front distortion are the principal in-field effects of atmospheric turbulence on laser beam propagation. Therefore, investigating beam coherence and phase-front distortion caused by turbulence in lab experiments provide the basis for creating intelligent algorithms and developing mitigation strategies.

Future research on specific turbulence reductions in physical atmospheres might benefit from the foundation provided by our current proposal. The paper presents the recommended modelling of turbulent eddies in particular turbulence regimes to understand the beam wander effect at various elevation angles. The outcome of the beam wandering in this regime appears to be consistent with prior simulated results [11,15]. Furthermore, in contrast to one Chi-Square model, the proposed Gamma model agrees with the analytical finding of beam wanders in a moderate turbulence domain.

In high and moderate turbulence regions, the link availability substantially decreases. Using an aperture averaging effect, or having a larger aperture area at the receiver, is one method of making up for it. Nevertheless, this results in a trade-off



by adding extra background noise to the system. Even so, the impact of background noise can be reduced by utilizing an expensive adaptive optics approach [20], a high-order pulse position modulation (PPM), or an optical heterodyne receiver [21]. With some additional system complications, the optical regenerate-and-forward (ORF) approach in a multi-hop system can significantly reduce the influence of background noise [22].

A new mechanism for simulating turbulence-induced beam wander in the laboratory environment was proposed. It tests various hypotheses over an experimental connection longer than 200 meters. In the atmospheric turbulence channel, where there is a temporal connection in the movement of the beam, the proposed resultant models could effectively replicate the effects of memory.

The recommended experiments could clarify how the model may be used to predict the generation of crosstalk in mode division multiplexing (MDM) systems using orbital angular momentum (OAM). In addition, the feature of precisely modelling the received intensity distribution and the temporal evolution of the received intensity is recommended. The development of improved signal processing and error correction methods for free-space optical communications, not previously achievable, may now be possible by our paradigm backed by a deep artificial network.

Worth mentioning, more than one new simulation tool has been developed and some of them are under upgrading for the understanding of atmospheric turbulence. Therefore, the deep enhancement of the PILab code simulation structure could help to generate further reliable and solid results of atmospheric turbulence-induced multiple and overlapping effects of laser beam spreading, wandering and scintillation.

## REFERENCES

- [1] Roggemann, Michael C., Byron M. Welsh, and Bobby R. Hunt, "Imaging through turbulence". CRC press, 1996.
- [2] Porfirev, Alexey P., Mikhail S. Kirilenko, Svetlana N. Khonina, Roman V. Skidanov, and Victor A. Soifer. "Study of propagation of vortex beams in aerosol optical medium." *Applied Optics* 56, no. 11, 2017: E8-E15.
- [3] Chauhan, Nikunj R., and Mehul K. Vala. "System design and performance analysis on the free space optics (FSO) system in atmospheric turbulence." *International Research Journal of Engineering and Technology (IRJET)* 4, no. 4, 2017.
- [4] Ferlic, Nathaniel A., Miranda van Iersel, Daniel A. Paulson, and Christopher C. Davis. "Propagation of Laguerre-Gaussian and Im-Bessel beams through atmospheric turbulence: A computational study." In *Laser Communication and Propagation through the Atmosphere and Oceans IX*, vol. 11506, pp. 97-112. SPIE, 2020.
- [5] Niaz, Ambreen, Farhan Qamar, Mudassar Ali, Romana Farhan, and Muhammad Khawar Islam. "Performance analysis of chaotic FSO communication system under different weather conditions." *Transactions on Emerging Telecommunications Technologies* 30, no. 2 (2019): e3486.
- [6] Raj Anthonisamy, Arockia Bazil, Padmavathi Durairaj, and Lancelot James Paul. "Performance analysis of free space optical communication in open-atmospheric turbulence conditions with beam wandering compensation control." *IET Communications* 10, no. 9 (2016): 1096-1103.
- [7] Nor, Norhanis Aida Mohd, Zabih Ghassemloooy, Jan Bohata, Prakriti Saxena, Matej Komanec, Stanislav Zvanovec, Manav R. Bhatnagar, and Mohammad-Ali Khalighi. "Experimental investigation of all-optical relay-assisted 10 Gb/s FSO link over the atmospheric turbulence channel." *Journal of Lightwave Technology* 35, no. 1, 2016: 45-53.
- [8] Andrews, L.C., Phillips, R.L.: "Optical turbulence in the atmosphere", in Pepper, E., (Ed.): "Laser beam propagation through random media" (SPIE Press, Washington, 2005), pp. 57-82.
- [9] Ghasemi, A., Abedi, A., Ghasemi, F., "Selected topics in radio wave propagation" in "Propagation engineering in wireless communications" (Springer, Switzerland, 2011, 2nd edn., 2016), pp. 403-427.
- [10] Mukherjee, Arka, Subrat Kar, and Virander Kumar Jain., "Analysis of FSO link under atmospheric turbulence from first principle." In *Optics and Photonics Japan*, p. 30aOD6. Optica Publishing Group, 2017.
- [11] Firoozmand, M., Moghadasi, M.N.: "Modeling and simulation of fading due of atmospheric turbulence by chi-squared and exponential pdf for a FSO link", *NNGT Int. J. Net. Comput.*, 2015, 2, pp. 1-9.
- [12] Mukherjee, Arka, Subrat Kar, and Virander Kumar Jain. "Analysis of beam wander effect in high turbulence for FSO communication link." *IET Communications* 12, no. 20 (2018): 2533-2537.
- [13] Latsa Babu, P., Srinivasan, B., "Characterizing the atmospheric effects on laser beam propagation for free space optical communication", *National Conf. on Communications, India*, 2008, pp. 332-334.



- [14] Fante, R.L., "Electromagnetic beam propagation in turbulent media", *Proc. IEEE*, 1975, 63, pp. 1669–1692.
- [15] Ishimaru, A. "Strong fluctuation theory", in "Wave propagation and scattering in random media", vol. 2 (Academic Press, New York, 1978), pp. 407–460.
- [16] Dios, F., Rubio, J.A., Rodríguez, A., et al., "Scintillation and beam-wander analysis in an optical ground station-satellite uplink", *Appl. Opt.*, 43, (19), pp. 3866–3873, 2004.
- [17] Reclons, J., Andrews, L.C., Phillips, R.L., "Analysis of beam wander effects for a horizontal-path propagating Gaussian-beam wave: focused beam case", *Opt. Eng.*, 46, (8), pp. 086002-1–086002-11, 2007.
- [18] Aljuboori, Haider M., and Dirk Giggenbach. "Design of Computer Identification System for GEO Satellite Link Characterization.", *Journal of Al-Ma'moon College*, 25, 2015.
- [19] Horwath, Joachim, Nicolas Perlot, Dirk Giggenbach, and Ralf Jungling. "Numerical simulations of beam propagation through optical turbulence for high-altitude platform crosslinks." In *Free-Space Laser Communication Technologies XVI*, vol. 5338, pp. 243-252. SPIE, 2004.
- [20] Kaushal, H., Kaddoum, G.: 'Optical communication in space: challenges and mitigation techniques', *IEEE Commun. Surv. Tutor.*, 19, (1), pp. 57–96, 2017.
- [21] Kopeika, N.S., Bordogna, J.: 'Background noise in optical communication systems', *Proc. IEEE*, 58, (10), pp. 1571–1577, 1970.
- [22] Kazemlou, S., Hranilovic, S., Kumar, S.: 'All-optical multi-hop free-space optical communication systems', *J. Lightwave Tech.*, 29, (18), pp. 2663–2669, 2011.